

Reprinted from

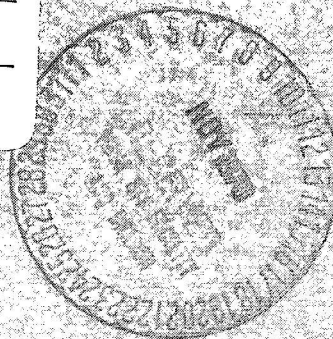
The Journal of
PHYSICS and
CHEMISTRY
OF SOLIDS

An International Journal

N 71-70785
TMX

FACILITY FORM 602

N 71-70785	(ACCESSION NUMBER)	(THRU)
11	(PAGES)	(CODE)
TMX-66579	(NASA CR OR TMX OR AD NUMBER)	(CATEGORY)



PERGAMON PRESS

OXFORD • LONDON • NEW YORK • PARIS

SQT-63097

PHOTOEFFECTS AND RELATED PROPERTIES OF SEMICONDUCTING DIAMONDS*

C. JOHNSON,[†] H. STEIN,[‡] T. YOUNG,[§] J. WAYLAND^{||} and W. LEIVO

Research Foundation and Physics Department, Oklahoma State University,
Stillwater, Oklahoma

(Received 31 January 1964; in revised form 28 February 1964)

Abstract—A number of properties of natural semiconducting diamonds have been investigated. The studies were concerned with the optical transmission, photoconductivity, mobility and activation energies of carriers, also the lifetimes and trapping of carriers. Optical transmission as a function of the temperature was measured in the region $200\text{ m}\mu$ – $13\text{ }\mu$. Optical absorption characteristic of type IIb diamond was observed at 2.43 , 3.40 , 3.56 and $4.07\text{ }\mu$ with slight peaks elsewhere; in other respects the absorption was similar to that of a type IIa diamond. Photoconductivity was determined as a function of excitation wavelength, intensity of illumination, temperature and electric field strength. A number of maxima in photoconductivity occur in the visible and near infrared ranges which are not resolved in the optical transmission measurements. The photoconductivity increases with increasing temperature until approximately 400°K after which it decreases. The maxima become better resolved and shift to shorter wavelengths with decreasing temperature. The long wavelength side of the photoconductivity in the range $0.4\text{ }\mu$ to $2.4\text{ }\mu$ may correspond to an acceptor level at 0.52 eV . Hall measurements show p -type conductivity with a room temperature hole mobility of $1300\text{ cm}^2/\text{V sec}$. Assuming a specific model and using the Hall data, an activation energy of 0.35 eV can be obtained. This corresponds to the optical absorption at 0.35 eV , and it is in agreement with temperature resistivity measurements. Lifetimes and trapping times of carriers were determined by various methods. A number of lifetimes and/or recombination times ranging from $9\text{ }\mu\text{ sec}$ to 84 min were obtained.

1. INTRODUCTION

THE optical and electrical properties of natural diamonds vary considerably from specimen to specimen. In fact, the continuous variation of the characteristics to several extremes was the origin of the general classification into the three general groups—type I, type IIa and type IIb. The early classification of diamonds into types I and II was mainly determined by their optical absorption. The type II diamonds transmit light further into

the ultraviolet range than do the type I, also the type I diamonds have optical absorption near $9\text{ }\mu$ which is not present in type II diamonds. In 1952 CUSTERS⁽¹⁾ discovered a rare type diamond which could conduct an electrical current but which otherwise had the characteristics of type II diamonds. Thereupon, Custers separated the type II class into types IIa and IIb. Types I and IIa diamonds are good insulators and type IIb are conductors of electricity.

The optical absorption of types I and IIa diamonds had been studied extensively for many years previous to the discovery of the type IIb diamonds. The origin of much of the optical absorption in types I and IIa diamonds is gradually becoming understood. SMOLUCHOWSKI and LEIVO examined a type IIb diamond (diamond DS-1 in this report) and found that it behaved as an extrinsic semiconductor.⁽²⁾ The plot of $k \ln \rho$ against $1/T$ gave a slope of 0.35 eV where k is the

* This research was supported in part by the U.S. Air Force Office of Scientific Research and the U.S. Air Force Cambridge Research Laboratories.

[†] Present address: National Aeronautics and Space Administration, Goddard Space Flight Center, Washington, D.C.

[‡] Present address: Sandia Corporation, Albuquerque, New Mexico.

[§] Present address: International Business Machines Corporation, Endicott, New York.

^{||} Present address: Eglin Air Force Base, Florida.

Boltzmann constant, ρ the resistivity and T the absolute temperature. Hall measurements showed a p -type conductivity. There have been many recent investigations of type IIb diamonds.⁽³⁾ The unavailability of diamonds with carefully controlled impurities and the very rare occurrence of natural type IIb diamonds complicates the investigation of the electrical and optical properties.

In order to correlate various effects, it was considered desirable to investigate a number of inter-related properties in the same semiconducting specimens. Reported herein are studies of the optical absorption, temperature dependence of photoconductivity, lifetimes and trapping of carriers and the mobility of carriers in natural semiconducting diamond. The diamonds used in the investigations are of type IIb and originated in the Premier Mine, South Africa. One diamond (diamond DS-2) is cut to rectangular dimensions of $2.3 \times 3.5 \times 6.5$ mm. Diamond DS-2 is blue on one end and nearly free from coloration on the other end. All the other diamonds are blue diamonds.

2. EXPERIMENTAL PROCEDURE AND RESULTS

2.1 Optical absorption

The infrared absorption measurements were obtained with Perkin-Elmer Spectrophotometers Models 12C and 21, and a Beckman Model IR-4. The near-infrared, visible and ultraviolet absorption spectra were taken on Beckman Spectrophotometers Models DK-1 and DK-2. The IR-4 has a resolution of 0.01μ at 10μ , and the DK-2 has a resolution of 2 \AA at $220 m\mu$. The temperature of the diamond was lowered by passing dry nitrogen through a liquid nitrogen bath and then around the diamond which was mounted in a

metal cryostat. The cryostat was equipped with quartz windows for the visible and ultraviolet regions and with sapphire windows for the infrared region. The temperature was increased in the same manner, the liquid nitrogen bath being replaced by a furnace. The temperature of the diamond was determined to within $\pm 2^\circ\text{C}$ with a thermocouple.

The absorption characteristics of diamond DS-2 are shown in Figs. 1-6. Changes in absorption with temperature are shown in Figs. 3-6. The

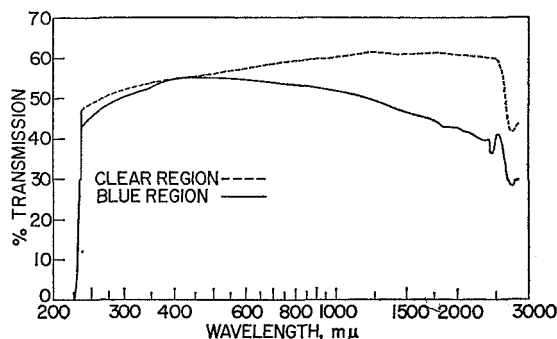


FIG. 1. Optical transmission of diamond DS-2 for two separate parts of the specimen.

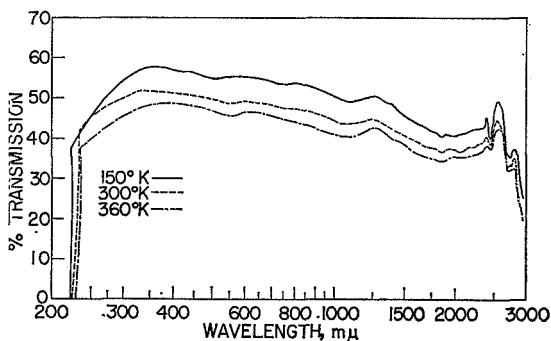


FIG. 3. Temperature dependence of the optical transmission of diamond DS-2.

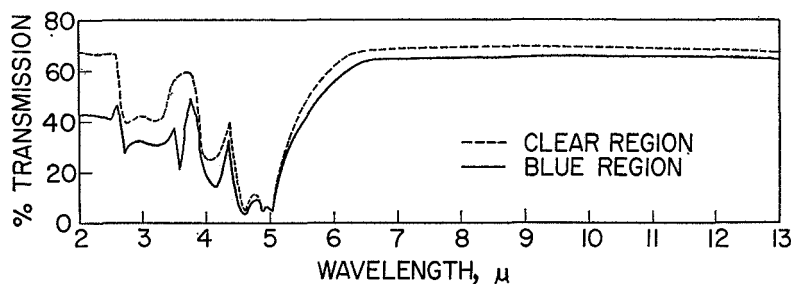


FIG. 2. Optical transmission of diamond DS-2 for two separate parts of the specimen.

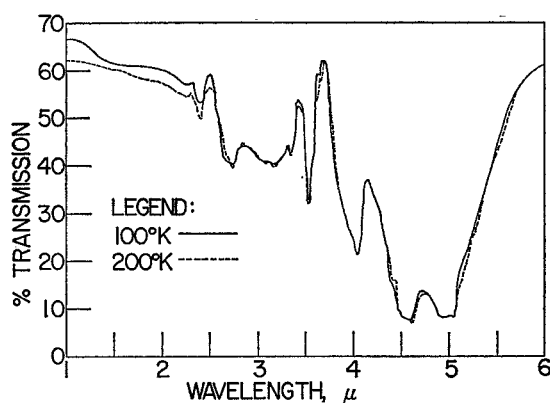


FIG. 4. Temperature dependence of the optical transmission of diamond DS-2.

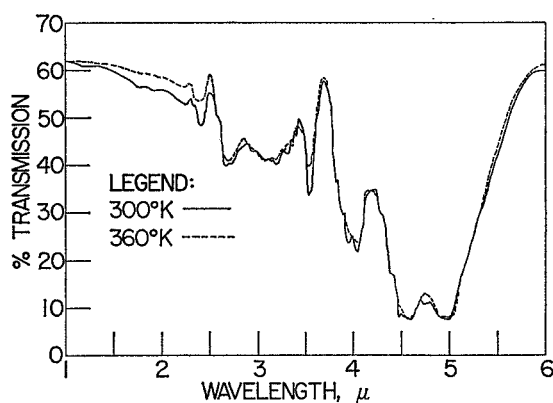


FIG. 5. Temperature dependence of the optical transmission of diamond DS-2.

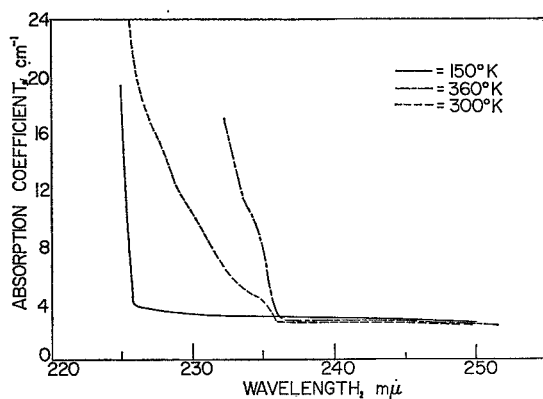


FIG. 6. Temperature dependence of the absorption coefficient of diamond DS-2 in the region of the fundamental absorption.

blue end of diamond DS-2 exhibits optical absorption bands in the 1–4 μ region which are not normally associated with a type IIa diamond. Maxima of the special absorption occur at 2.43, 3.40, 3.56 and 4.07 μ , with slight peaks elsewhere. The clear end exhibits absorption which is nearly that of type IIa diamonds. Room temperature resistivities using a four probe method are $3.6 \times 10^5 \Omega\text{-cm}$ for the clear end and $65 \Omega\text{-cm}$ for the blue end. The characteristic absorption in the blue end increases with decreasing temperature. Decreasing the temperature to 150°K changes the wavelength at which the ultraviolet absorption starts to become significant from 236 to 226 $m\mu$; however, the wavelength at which extinction occurs remains nearly unchanged (Fig. 6). Increasing the temperature to 360°K does not change the wavelength at which the ultraviolet absorption starts to become significant, but it shifts the extinction wavelength from 225 to 231 $m\mu$. Diamond DS-1 shows the same absorption peaks as the blue end of diamond DS-2.

The curves have been adjusted for continuity when changing detectors or light sources. As such, the value of the percent transmission cannot be taken as absolute. The discontinuity in the transmission curve can arise from the following causes: First, light beam is not uniform in intensity and adjusting the focus shifts the region of maximum intensity to different parts of the diamond which is not homogeneous with regard to optical absorption. Second, the detectors may not give uniform response over their surfaces. If the diamond does not have exactly parallel faces the energy may be incident on a different area of the detector after passing through the diamond than the area used in establishing the 100 per cent transmission.

The birefringence of the diamond was also examined. The birefringence pattern in the blue part of diamond DS-2 is different from the pattern in the clear region. The clear end exhibits parallel streaks similar to those observed by RAMAN and JAYARAMAN in what were probably type II diamonds.⁽⁴⁾ The blue end of diamond DS-2 exhibits a cross-hatched pattern.

2.2 Photoconductivity

Photoconductivity in semiconducting diamond was studied as a function of intensity of illumination, spectral distribution, electric field strength

and temperature. It was found that the semiconducting diamonds, besides being photoconducting in the ultraviolet, have a number of photoconducting maxima in the visible and infrared regions.

Photocurrents were measured with a Beckman DK-1 spectrophotometer which was altered to record photocurrents directly. A tungsten lamp was used for the visible and near infrared source and a hydrogen lamp for the ultraviolet source. The light was chopped at 480 c/s. The spectral distribution of the tungsten light source was determined using a vacuum thermopile with a quartz transmission window. The curve of the spectral distribution at the crystal surface is shown in Fig. 7. The ultraviolet spectral response curve was obtained indirectly with a General Electric FJ-76 phototube. The diamond was placed in the regular sample compartment of the DK-1 spectrophotometer and was shielded from stray radiation. The recorder was calibrated by applying known differences in potential to the amplifiers thus making it possible to record photocurrents directly. The spectral response curves of the photoconductivity in the diamond are reduced to photocurrent per incident photon per second.

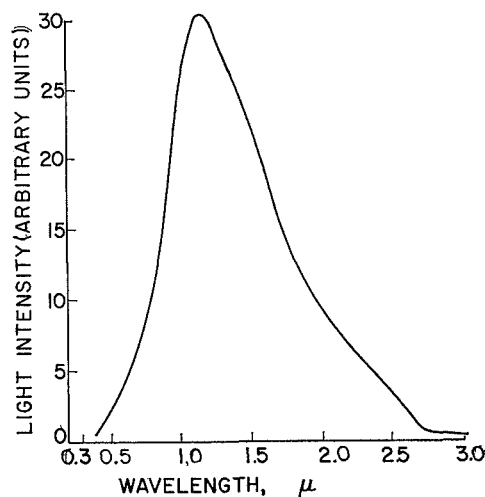


FIG. 7. Intensity distribution of the tungsten light source at the exit slit of the monochromator.

The crystal holder for low temperature measurements consisted of a double-walled evacuated container with quartz windows. Sodium chloride

windows were used for infrared measurements. The cooling for low temperature work was obtained by passing dry nitrogen through a liquid nitrogen bath and then into the inner container. The currents measured were of the order of 10^{-10} A. Although photoconductivity measurements were made on other semiconducting diamonds with similar results, the results given here were obtained on specimen (DS-2).

2.2(a) *Dependence of photocurrent upon intensity of illumination.* The dependence of the photocurrent in diamond DS-2 was determined as a function of the intensity of the radiation at constant wavelength. It was found that the photocurrent depends linearly upon the intensity of the radiation. A typical curve is shown in Fig. 8. In this case the excitation wavelength was $600 \text{ m}\mu$ and the maximum photocurrent was approximately 10^{-7} A.

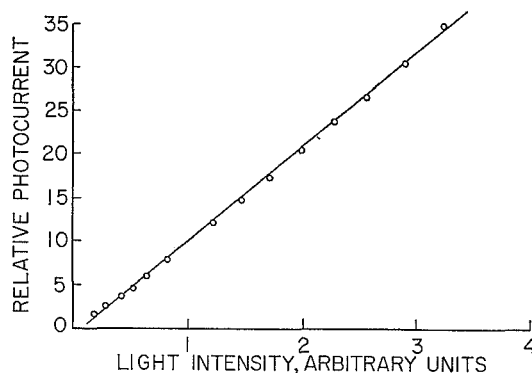


FIG. 8. Dependence of the photocurrent in diamond DS-2 upon the intensity of irradiation.

Ultimately the sensitivity of a photoconductor is not measured by the current per photon but by the signal to noise ratio for a given amount of incident radiation.⁽⁵⁾ A good signal to noise ratio can be obtained in the clear end of the diamond at room temperature because the resistivity of this end is such that an appreciable field can be obtained without a very large dark current. A large dark current introduces an appreciable amount of noise. The major source of noise originates with the contacts and is dependent upon the electric field direction. Reverse bias, which occurs when the blue end is negative, introduces a large amount of noise. With forward bias, the noise level is considerably lower, and direct illumination of either

or both of the contacts does not add to the noise level of the photocurrent.

2.2(b) Dependence of photocurrent upon electric field strength. The dependence of the photocurrent with electric field strength was studied in order to determine the presence of potential barriers in the crystal. The photocurrent is a linear function of the field in the measured range. The field was measured using potential probes, thus eliminating the potential drop across the contacts.

2.2(c) Spectral response of photocurrent as a function of temperature. The spectral response of the photoconductivity was determined in the wavelength range $0.200\text{--}20\text{ }\mu$ at various temperatures between 127 and 450°K . Figure 9 shows the spectral distribution of the photocurrent in the visible range at room temperature. The curve gives the photocurrent per incident photon/sec vs. the wavelength in microns. Upon increasing the sensitivity of the circuit to a maximum and opening the

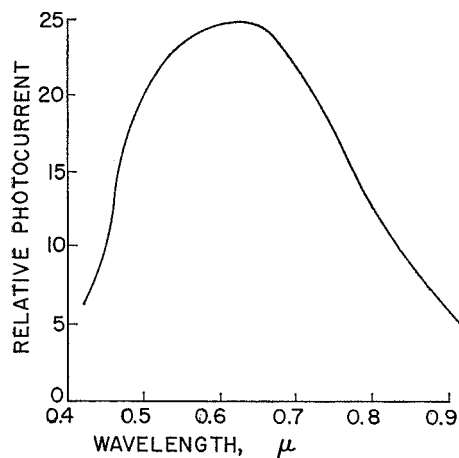


FIG. 9. Spectral distribution of the photocurrent in diamond DS-2 at room temperature. The ordinate is proportional to the photocurrent per incident photon/sec.

slit to 2 mm , additional peaks were found at 1.46 and $1.75\text{ }\mu$. The peaks are very weak at room temperature but assume a major role at a low temperature as will be discussed later. A weak photocurrent is obtainable in the region $3.0\text{--}3.5\text{ }\mu$. No photoconductivity was detected in the regions $5.1\text{--}12\text{ }\mu$, or $0.245\text{--}0.350\text{ }\mu$.

Increasing the temperature increases the photocurrent up to approximately 400°K . At higher temperatures the photocurrent decreases as the temperature increases. It should be noted that the increase is an increase in the photocurrent of the broad region of photoconductivity from 0.35 to $3\text{ }\mu$, and the half-width is not appreciably increased. The noise level rises sharply at 405°K and increases rapidly with increasing temperature.

The maximum value of the photocurrent decreases in magnitude and shifts to shorter wavelengths upon decreasing the temperature below 300°K . The shift is already observable at a temperature of 250°K (Fig. 10) with the predominant peak appearing at 0.590 instead of $0.600\text{ }\mu$. At 223°K an additional peak is resolved at $1.24\text{ }\mu$,

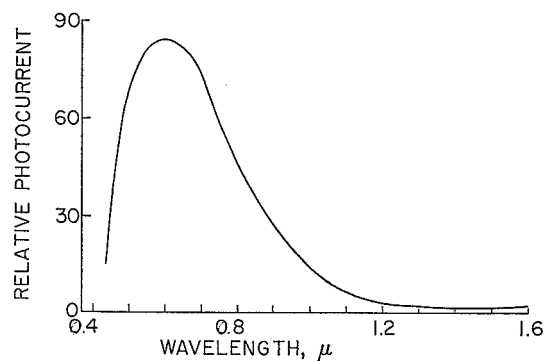


FIG. 10. Spectral distribution of the photocurrent in the visible and near infrared regions at 250°K for diamond DS-2.

and the predominant peak shifts to $0.58\text{ }\mu$ (Fig. 11). The ultraviolet induced photocurrent is no longer measurable from approximately 240°K and lower. When the temperature is reduced to 150°K the predominant peak shifts to $0.52\text{ }\mu$. In addition, new peaks appear at 1.02 , 1.62 and $2.18\text{ }\mu$ (Fig. 12). There is a slight indication of a peak at $1.24\text{ }\mu$ in the curve which does appear at other temperatures. At a temperature of 127°K , the lowest temperature attained in this study of photoconductivity, the largest peak occurs at $0.88\text{ }\mu$. The peak which appears at $0.6\text{ }\mu$ at 300°K and which shifts to $0.52\text{ }\mu$ at 150°K has now disappeared; therefore, the region is not shown in Fig. 13. The photoconductivity in the ultraviolet region has been previously reported (last paper under reference (3)).

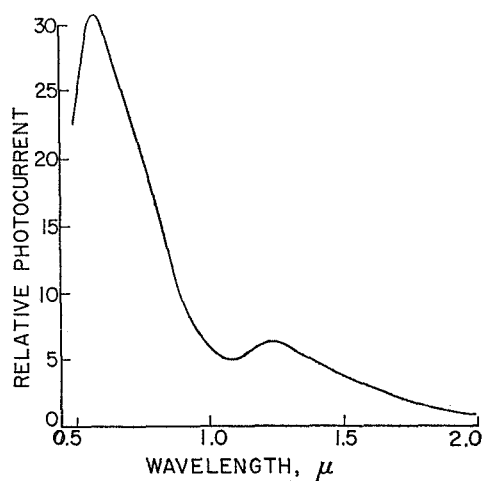


FIG. 11. Spectral distribution of the photocurrent for diamond DS-2 at 223°K.

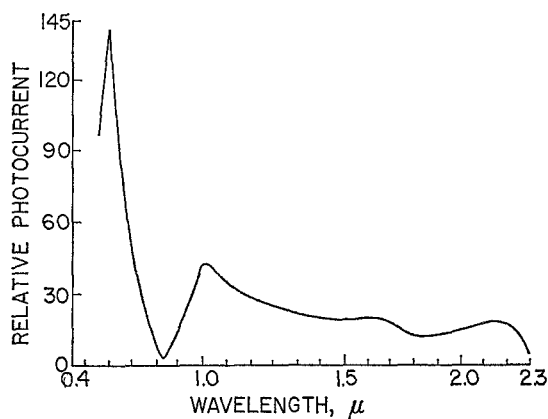


FIG. 12. Spectral distribution of the photocurrent for diamond DS-2 at 150°K.

2.2(d) *Surface vs. bulk photoconductivity.* Measurements were made to determine whether the conduction process is a bulk or a surface phenomenon. The diamond was masked and irradiated in such a manner that the ratio of the volume to the surface area was different. The photocurrent was the same regardless of which face was illuminated thus indicating a bulk effect. Next, the diamond was masked except for small areas on different faces, and these areas were irradiated. The ratio of the photocurrents was in closer agreement with the ratio of the volumes irradiated than the ratio of the surface areas. This again indicates a bulk

effect, but the ratios were not exact. Next, the diamond was masked except for thin strips along the edges. In this case the ratio of the photocurrent was in closer agreement with the ratio of the surface areas rather than the ratio of the volumes. This can possibly be explained by internal reflections from the side surfaces. Although surface conduction cannot be ruled out, from the data taken one must consider that the conduction process is primarily a bulk phenomenon.

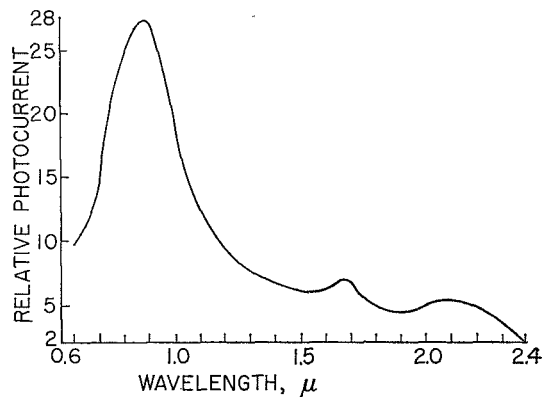


FIG. 13. Spectral distribution of the photocurrent for diamond DS-2 at 127°K.

2.3 Lifetimes and trapping of carriers

The generation and decay of carriers responsible for photoconductivity in semiconducting diamonds were studied under varying conditions. The general methods which have been previously employed to study lifetimes and trapping in semiconductors were tried. These include the photoelectromagnetic effect, diffusion length techniques, and photocurrent growth and decay methods. Of the methods tried, only the photocurrent growth and decay gave useful results. Diamond, with an energy gap of 5.6 eV, provides a broader range in which to study intermediate states than do other semiconductors; however, the large energy gap leads to other difficulties. In particular, it is difficult to obtain good data in the fundamental absorption range because of the lack of a suitable intense source of radiation in the ultraviolet region.

From the curves of photocurrent vs. excitation wavelength (Figs. 12 and 13), it is seen that several centers may be responsible for the photocurrent. A study was made of the rate of rise and

decay of the photocurrent as a function of the wavelength. In the visible region of the spectrum a tungsten lamp in conjunction with a monochromator was used to excite the photocurrent. The excitation ranged from steady illumination used to determine the steady-state build-up and decay to very short pulses obtained with a camera shutter and chopping disc arrangement. The ultraviolet region was studied using a mercury arc, a hydrogen arc, and short duration sparks. The spark source consisted of a high voltage power supply and a pulse-forming network. The pulse-forming network was discharged between metal electrodes producing an intense short pulse of light which contained a large amount of radiation in the fundamental absorption region of the diamond. The pulse duration was varied by changing the delay line and adjusting the high voltage power supply.

When the sample was exposed to the whole spectrum of the tungsten light decay times of 30 and 39 min were obtained. Using short pulses of light, various recombination times were obtained. The response and decay times of the photocurrent were found to be dependent upon the exciting wavelength. This is attributed to the many intermediate energy levels present in the energy gap of the diamond. Recombination time as used here is the time required for the photocurrent to attain $1/e$ of its steady state value from the initial time of cutoff of the radiation source. Excitation with 222 m μ radiation resulted in a 12 and an 84 min decay; 440 m μ produced a 30 min decay and 630 m μ a 6 min decay. With 800 m μ radiation, decays of 30 sec and 7 min occurred.

The response time of the photocurrent produced by a short intense spark of light was 10 μ sec. The response of a photocell to the same light source was approximately 1 μ sec. The difference between the build-up time of the photocurrent of the diamond and the response time of the photocell is taken to be very close to the free carrier lifetime in the diamond. A free carrier lifetime of 9 μ sec is therefore obtained in the particular diamond (DS-2) used in this study. The lifetime obtained in this case is believed to be largely independent of trapping.

A detectable photoelectromagnetic effect could not be produced in the sample. This is believed to be due to a very high surface recombination

rate and the lack of an intense source in the ultraviolet region. Similarly, diffusion length experiments gave no useful results.

2.4 Hall effect studies

Studies of the Hall effect were undertaken in order to obtain information on the density and mobility of the carriers and also to get some idea of an effective mass of the carriers which would be consistent with a speculative model for the system. The conductivity was due to holes with a room temperature value for the mobility of 1300 cm²/V-sec.

Hall effect measurements were carried out with specimen DS-2 in the temperature range from room temperature to 527°C. There was no measurable Ettingshausen effect, and the voltage measured was essentially the Hall voltage. Figure 14 is a plot of the logarithm of the product of the Hall coefficient and the absolute temperature to the three-halves power versus the inverse of the absolute temperature. From the slope of the curve in the low temperature range an activation energy of 0.35 eV is obtained. It should be remembered that this cannot be taken with certainty as the activation energy because a specific model for the imperfection states was assumed, and therefore the true position of the Fermi level is uncertain.

A simple model was considered which contains one acceptor and one donor level with the acceptor level located at 0.35 eV. Substituting values for temperature and the corresponding density of holes in the equation

$$p = 3 \left(\frac{N_a - N_d - p}{N_d + p} \right) \left(\frac{2\pi m^* kT}{h^2} \right)^{3/2} e^{-\epsilon/kT} \quad (1)$$

gives three equations in three unknowns, N_a , N_d , and m^* . The symbols are the standard ones. The problem was solved by graphical means. Values for N_a , N_d and m^* were substituted in equation (1), and the density of the carriers was plotted as a function of the absolute temperature. A series of the theoretical curves was compared with the curve obtained experimentally until a good agreement was reached. Good agreement was obtained when the effective mass was 0.3 electron mass.

Equation (1) is based on the condition that the density of electrons in donor states is negligible compared to the density of holes. The factor three

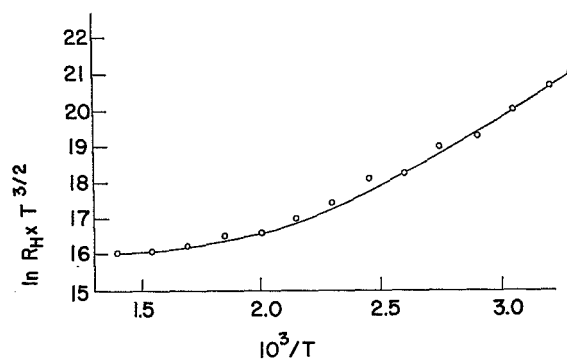


FIG. 14. Hall coefficient times $T^{3/2}$ as a function of the inverse absolute temperature for diamond DS-2.

in the equation arises from the degeneracy of the levels at the top of the valence bands. In the case of diamond the valence band edge occurs at the center of the Brillouin zone and consists of three bands touching at the central point if spin-orbit coupling is neglected.⁽⁶⁾ The spin-orbit interaction should be very small (~ 0.005 eV). The assumption of threefold degeneracy at the top of the valence band and spherical energy surfaces introduces the factor three in the equation.

3. DISCUSSION

From the optical absorption, photoconductivity, and other studies it is apparent that there are a host of energy levels of various types in the energy gap of a natural semiconducting diamond. The optical absorption shown in Figs. 1–6 is for specimen DS-2 which has proved to be interesting in many respects. The specimen being a large parallelepiped is well suited for optical measurements. One end of the specimen is light blue, and the other end is clear to the eye, but the specimen is a single crystal from X-ray analysis. Both regions are semiconductors with the blue region having a room temperature resistivity of $65 \Omega\text{-cm}$ and the clear region $10^5 \Omega\text{-cm}$. Figures 1 and 2 give the optical absorption for the two regions separately. It can be seen that the optical absorption in the clear region approaches that of a type IIb diamond, whereas the blue end shows the extra absorption at 2.43 , 3.40 , 3.56 and 4.07μ along with other small peaks which is characteristic of type IIb

diamonds. The demarcation line between the blue and the clear regions is quite sharp, and the birefringence patterns are different in the two regions. It is conceivable from observations of the birefringence patterns that single slip has occurred in the clear region of the diamond and double slip in the blue region. Evidence of slip has been observed in diamonds by TOLANSKY.⁽⁷⁾ Double slip could be more effective in generating vacancies than single slip. In the case of the alkali halides, upon the onset of double slip the rate of generation of vacancies with strain is greatly increased.⁽⁸⁾ This could indicate that the imperfections responsible for the conductivity could be related to a lattice imperfection or possibly an impurity atom associated with a lattice imperfection other than as a direct substitutional impurity. The optical absorption at 3.56μ which corresponds to 0.35 eV does agree with the acceptor activation energy of 0.35 eV obtained from the temperature-resistivity curves.⁽²⁾ The determination of activation energies from the temperature-resistivity curves does involve an assumption about the location of the Fermi-level which is actually unknown. WENTORF and BOVENKIRK⁽⁹⁾ produced semiconducting diamonds by diffusing in small amounts of boron, beryllium, or aluminum. Of the three only boron produced a blue color. However, they obtained a value of 0.17 – 0.18 eV from the slope of the resistivity-temperature curves rather than 0.35 eV obtained for diamond DS-2 and also obtained by others in natural semiconducting diamonds. As such, possibly a lattice defect associated with a Group III impurity is responsible for the 0.35 eV level.

The low energy side of the absorption edge of diamond DS-2 (Fig. 6) shifts 0.23 eV between 150 and 360°K compared with an expected change in the energy gap of 0.04 eV. This is indicative of phonon assisted transitions in agreement with CLARK.⁽¹⁰⁾ The optical absorption beyond 0.6μ (Fig. 1) is greater in the region which appears blue to the eye and accounts for the visually observed blue color. The broad region of absorption from 0.6 to 2.8μ is not resolved in the optical measurements, but the photoconductivity measurements (Fig. 13) show a number of maxima in this region.

Photoconductivity studies were undertaken to aid in establishing the positions of energy levels in the energy gap. Since the conductivity is p -type,

photoionization levels using visible and infrared radiation would correspond to ionization of a hole from a bound state. The presence of a number of maxima in the photoconductivity is similar to the case of germanium.⁽¹¹⁾ The present problem of compensating acceptor levels in diamond with known donors makes it difficult to identify a level with a particular imperfection.

The observations on the temperature dependence of the photocurrent show that the photocurrent increases with temperature until approximately 400°K after which it decreases with increasing temperature. Photocurrents in other materials have been observed both to increase and decrease with temperature depending on the temperature range and the light intensity.⁽⁵⁾ The temperature can be expected to influence the lifetimes of free carriers through the capture cross sections and the number of ground states. Since the distances of the quasi Fermi-levels from the valence and conduction bands depend on the temperature, the higher temperature would bring the levels closer together. If one class of bound states were predominant, this would reduce the number of ground states and result in an increase in photocurrent with increasing temperature. When there is more than one class of bound states, the photocurrent can increase or decrease with change in temperature as different bound states move in or out of a ground state category.

Part of the optical absorption in the 2–4 μ range may be due to transitions of free holes between the valence bands which, although degenerate at $k = 0$, separate for $k \neq 0$. This absorption along with lattice absorption could compete with the transitions producing photoconductivity and thus produce the minima observed in the photoconductivity. Although there is observable photoconductivity in the 2.8–3.5 μ range it is weak compared to the photoconductivity in the 0.6–2.8 μ range. The long wavelength side (2.4 μ) of the photoconductivity in the range 0.4–2.4 μ (Fig. 13) may correspond to an acceptor level at 0.52 eV. This also appears in the optical absorption (Fig. 3) as a peak at 2.43 μ (0.51 eV). As seen from Fig. 3 the absorption at 2.43 μ is temperature dependent with the absorption increasing with decreasing temperature. A thermoluminescence level at 0.52 eV was obtained by HALPERIN and NAHUM.⁽¹²⁾

The photocurrent increases linearly with the applied electric field which is the more usual case with other photoconductors. Even though a potential barrier must exist between the blue and the clear regions of the diamond because of their different densities of holes, the barrier is such as to not affect the linearity of the curve in the measured range.

The photocurrent produced by radiant energy in photoconductors in general may vary as a linear function of the light intensity or as a power different from unity. In some cases the increase in intensity decreases the lifetimes of the carriers, and therefore the photocurrent increases as a fractional power of the intensity.⁽⁵⁾ Figure 8 shows that the photocurrent increases linearly with the intensity of the radiation, thus indicating the possibility of a uniform distribution of bound states or the presence of bound states with different cross sections.

The studies of lifetimes and trapping times show the presence of many long lifetime traps. Therefore, care must be taken in interpreting experiments involving equilibrium conductivity data. Although the longest trapping time measured was 84 min there is evidence of trapping times of over one day.

The determination of an activation energy of 0.35 eV from the Hall data is in agreement with the 0.35 eV obtained from temperature-resistivity measurements, and it also corresponds with the optical absorption at 0.35 eV. The value 0.3 electron mass obtained from Hall measurements for the effective mass of a hole can be compared with the 0.7 electron mass for the effective mass of a hole obtained from cyclotron resonance measurements.⁽¹³⁾ The determination of an effective mass from the Hall data is dependent upon the particular model which is chosen. General agreement as such is helpful in establishing reasonable models.

Acknowledgements—We thank Dr. J. F. H. CUSTERS, Research Consultant, Industrial Distributors (1946) Limited, South Africa, for the assistance he has given us in this work and for making several semiconducting diamonds available for our studies. We also thank Dr. GEORGE SWITZER of the U.S. National Museum for the loan of a semiconducting diamond.

REFERENCES

1. CUSTERS J. F. H., *Physica* **18**, 489 (1952); **20**, 183 (1954).
2. LEIVO W. J. and SMOLUCHOWSKI R., *Phys. Rev.* **98**, 1532 (1955).
3. BROPHY J. J., *Phys. Rev.* **99**, 1336 (1955); CUSTERS J. F. H., *Nature, Lond.* **176**, 173 (1955); AUSTIN I. G. and WOLFE R., *Proc. Phys. Soc., Lond.* **B69**, 329 (1956); CLARK C. D., DITCHBURN R. W. and DYER H. B., *Proc. Roy. Soc.* **A234**, 363 (1956); WOLFE R. and WOODS J., *Phys. Rev.* **105**, 921 (1957); CHARETTE J. J., *Physica* **25**, 1303 (1960); BELL M. D. and LEIVO W. J., *Phys. Rev.* **111**, 1227 (1958).
4. RAMAN C. V. and JAYARAMAN A., *Proc. Ind. Acad. Sci.* **A32**, 65 (1950).
5. ROSE A., *Proc. Inst. Radio Engrs.* **43**, 1850 (1955).
6. HERMAN F., *Phys. Rev.* **88**, 1210 (1952).
7. TOLANSKY S., *Phil. Mag.* **44**, 514 (1953).
8. VAUGHN W., LEIVO W. and SMOLUCHOWSKI R., *Phys. Rev.* **110**, 652 (1958).
9. WENTORF R. and BOVENKIRK H., *J. Chem. Phys.* **36**, 1987 (1962).
10. CLARK C. D., *J. Phys. Chem. Solids* **8**, 481 (1958).
11. BURSTEIN E., DAVISSON J., BELL E., TURNER W. and LIPSON H., *Phys. Rev.* **93**, 65 (1954).
12. HALPERIN A. and NAHUM J., *J. Phys. Chem. Solids* **18**, 297 (1961).
13. RAUCH C. J., *Phys. Rev. Lett.* **7**, 83 (1961).